

## Numerical study of encased stone columns subjected to embankment loading

M.S.S. Almeida, Graduate School in Research and Engineering (COPPE), Federal University of Rio de Janeiro (UFRJ), Rio de Janeiro, Brazil.

I. Hosseinpour, Department of Civil Engineering, Faculty of Engineering, University of Guilan (GU), Rasht, Iran.

M.C.F. Almeida, Program of Civil Engineering, School of Polytechnic, Federal University of Rio de Janeiro (UFRJ), Brazil.

T.N. Nikolaou, Program of Civil Engineering, School of Polytechnic, Federal University of Rio de Janeiro (UFRJ), Brazil.

P.A.C. Saggin, Program of Civil Engineering, School of Polytechnic, Federal University of Rio de Janeiro (UFRJ), Brazil.

### ABSTRACT

Granular columns encased with geosynthetic material are commonly used to reduce the total deformations and to improve the load carrying capacity of very soft soil deposits ( $s_u < 15$  kPa) underneath the embankments (Almeida et al. 2018). In this study a series of numerical analysis is performed using Plaxis 2D finite element code, aiming to investigate the influence of the encasement stiffness  $J$ , area replacement ratio  $a_c$ , coefficient of at-rest earth pressure  $K_0$ , and friction angle  $\phi_c$  of the column filling material on the settlement development and the column horizontal deformation (i.e. geotextile expansion). The data available from a full-scale load test is used to perform the finite element analyses on which geotextile-encased granular columns (GEC) stabilized 10 m-thick very soft soil (Almeida et al. 2015). Results of the parametric analyses showed that the increased friction angle of the column material reduced rather the geotextile expansion than the embankment settlement. Increasing either the encasement stiffness or the column diameter was also found to reduce remarkably both the settlement and the geotextile expansion. The differential settlements at the base and on the top of the test embankment were also compared while the area replacement ratio  $a_c$  changed. The results demonstrated that the differential settlement at base of the embankment was associated with  $a_c$  values.

### 1. INTRODUCTION

Compacted granular columns are one of the soft ground improvement method more commonly and successfully used to decrease the settlement, to increase the load carrying capacity and to accelerate the consolidation time of soft soils. In very soft clayey deposits ( $s_u < 15$  kPa) the granular columns could be wrapped by an appropriate geosynthetic material on which the additional confining support prevents column excessive bulging thus decreasing the total deformations and improving the load carrying capacity of the foundation soil (Raithel et al. 2002). In addition, the encasement prevents the intermixing of the granular material into the surrounding soil, subsequently the permeability of the granular columns remains constant. In recent years numerical analyses have been frequently used to study the behavior of the geotextile-encased columns (GEC) in soft soils (Murugesan and Rajagopal, 2006; Khabbazian et al. 2010; Almeida et al. 2013; Hosseinpour et al. 2014, 2016, 2017a; Geng et al. 2017).

The geotextile expansion (i.e. column bulging) is one of the critical aspect controlling the overall stability of the embankment over encased granular columns and has been less investigated in the previous researchers. Among the soil and column parameters analyzed, the soil coefficient of at rest pressure  $K_0$ , stiffness of the geosynthetic encasement  $J$ , frictional angle of the column material  $\phi_c$  and area replacement ratio  $a_c$  are those which affect significantly the behavior of the embankment over GEC system. This paper uses 2D numerical analysis to assess the influence of such parameters mentioned above on the variations of the settlement and geotextile expansion for a test embankment built over geotextile-encased granular columns. Numerical analyses are performed using a unit cell model for which an axisymmetric cylinder, consisting of a singular encased column and its surrounding soft soil, is analyzed. In addition, the critical height for the encased column supporting embankment is studied and compared with that proposed for embankment over rigid piles.

## 2. NUMERICAL SIMULATION

Data provided by a test embankment constructed on an improved soft soil was used for the numerical analysis (Almeida et al. 2015). Thirty-six geotextile-encased granular columns stabilized soft soil in a test area located in west of city of Rio de Janeiro, Brazil. The diameter and length of the granular columns were 0.8 m and 11 m, respectively. The granular columns were implemented in a square mesh with 2.0 m center to center spacing producing an area replacement ratio of  $a_c = 0.125$ . The soil profile at the test area was mainly characterized by a 10 m-thick very soft clay layer ( $s_u < 15$  kPa) limited to a 1.8 m-thick working platform on top. A 5.3 m-high test embankment, equivalent to 150 kPa total stress, was constructed over GEC system. The ground water level was on the top of the soft clay layer as observed in-situ. The embankment construction was performed in four stages along 65 days and then left in place for 180 days when about 80% of the excess pore pressures had already dissipated. The encased granular columns and the soft soil were carefully instrumented to record the in-service response of the test embankment.

Finite element analysis (FEA) was carried out using Plaxis 2D program (Brinkgreve and Vermeer, 2012) in order to take advantage of its capability for time-dependent soil consolidation problems. An axisymmetric unit cell was adopted for numerical modeling and the soil layering was selected based on the typical ground profile observed in-situ. The embankment sectional view and the unit cell model are shown in Figure 1. Considering boundary conditions, the model was free to deform vertically in both sides, while neither vertical nor horizontal displacements were allowed at the base. The geotextile encasement was modeled as an isotropic nonlinear geogrid element, available in Plaxis software, which has axial stiffness thus sustaining only tensile forces along the length. The nonlinearity properties of the geotextile encasement was considered by assigning an axial stiffness and ultimate tensile force. A fine coarseness finite element mesh was used with a local mesh refinement in the region close to the encasement. The steps of the calculation consisted of activating the clusters corresponding to the various embankment layers in order to simulate embankment construction followed by consolidation intervals between the stages to analyze the development and dissipation of the excess pore pressures in the saturated soft soil as a function of time. Elasto-plastic Mohr-Coulomb (MC) model was adopted for both the granular column and the embankment material; however soft clay layers were simulated using a Cam-Clay model (Soft Soil) for which the parameters were obtained from the site investigation (Hosseinpour et al. 2017b). The encasement material was woven geotextile simulated as a nonlinear material with tensile modulus and maximum tensile force equal to 1750 kN/m and 90 kN/m, respectively. There was also a biaxial geogrid reinforcement with  $J = 2200$  kN/m placed below the embankment. The other material properties are listed in Table 1.

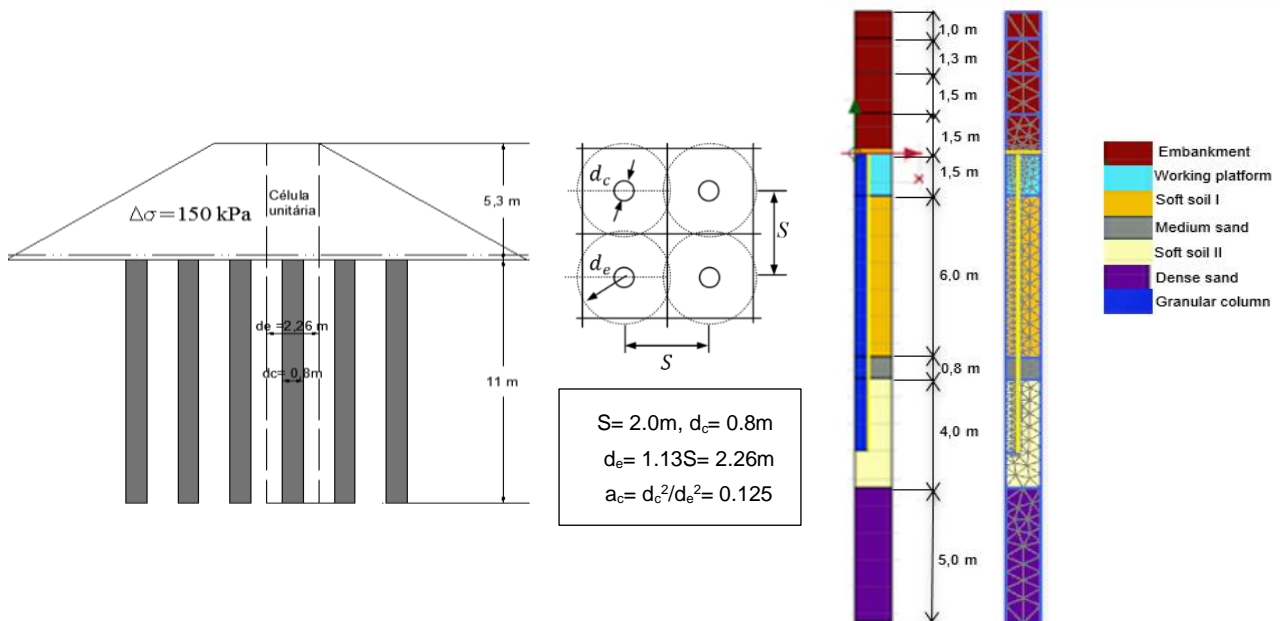


Figure 1. Embankment side view and unit cell adopted for numerical analysis.

Table 1. Material parameters used in numerical analysis of test embankment.

Material and constitutive model	$\gamma_{sat}$ (kN/m <sup>3</sup> )	$k_h$ (m/d)	$k_v$ (m/d)	$\phi'$ (°)	$c'$ (KPa)	$E'$ (MPa)	$C_c$ (-)	$C_s$ (-)
Embankment (MC)	28	1.0	1.0	45	0	53	.....	.....
Stone column (MC)	20	10.0	10.0	40	0	80	.....	.....
Soft clay I (SS)	14.4	$1.6 \times 10^{-5}$	$5.2 \times 10^{-6}$	26	4	1	0.98	0.084
Soft clay II (SS)	16.8	$9.7 \times 10^{-6}$	$4.8 \times 10^{-6}$	28	6	1.65	0.13	0.025
Medium sand (MC)	18.5	0.5	0.5	30	0	22	.....	.....
Dense sand (MC)	20	1.0	1.0	38	0	30	.....	.....
Working platform (MC)	19.7	0.6	0.6	33	3	12	.....	.....

$\gamma_{sat}$ = saturated unit weight;  $k_h$ = coefficient of horizontal permeability;  $k_v$ = coefficient of vertical permeability;  $\phi'$ = drained angle of friction;  $c'$ = drained cohesion;  $E'$ = drained stiffness,  $C_c$ = coefficient of compressibility;  $C_s$ = coefficient of swelling.

### 3. PARAMETRIC STUDY

#### 3.1 Influence of stone column friction angle

The parametric study was carried out by varying the values of the friction angle of the column filling material  $\phi_c$  within the range of values recommended in the literature (Almeida et al. 2018). The values chosen were 35°, 40° and 45°. Figure 2a shows the influence of the column's friction angle on settlement development below the embankment centerline. It is observed that the higher  $\phi_c$  reduces the magnitude of the settlement at any stage of embankment construction and post-construction. This is because the greater  $\phi_c$  increases the shear resistance of the encased column thus a lower embankment load is transferred to the soft clay subsequently the settlement reduces. The settlement difference between the friction angles of 35° and 40° is 52 mm and the settlement difference between the friction angles of 40° and 45° mm is 58 mm representing a reduction of about 10% of the magnitude of the settlements for an increase of 5% in the value of the friction angle.

The increased friction angle of the column filling material  $\phi_c$  reduces the lateral expansion of the geotextile since it increases the strength of the column material as discussed above. This variation can be verified in Figure 2b on which the measured geotextile expansion is compared with predicted values. Considering the column radius equal to 0.8 m, the radial strains at the end of monitoring time are determined as 2.93%, 1.96% and 1.12% respectively for  $\phi_c$  values equal to 35°, 40°, and 45°. These results indicated that an increase in column friction angle from 35° to 45°, reduces nearly 2.5 times the geotextile expansion (i.e. column bulging) thus preventing the column failure due to excessive bulging at high load circumstances. It is observed that, in general, the friction angle of the column  $\phi_c$  influences more efficiently the column bulging than the settlement below the embankment improving therefore the overall stability of the embankment over encased stone columns.

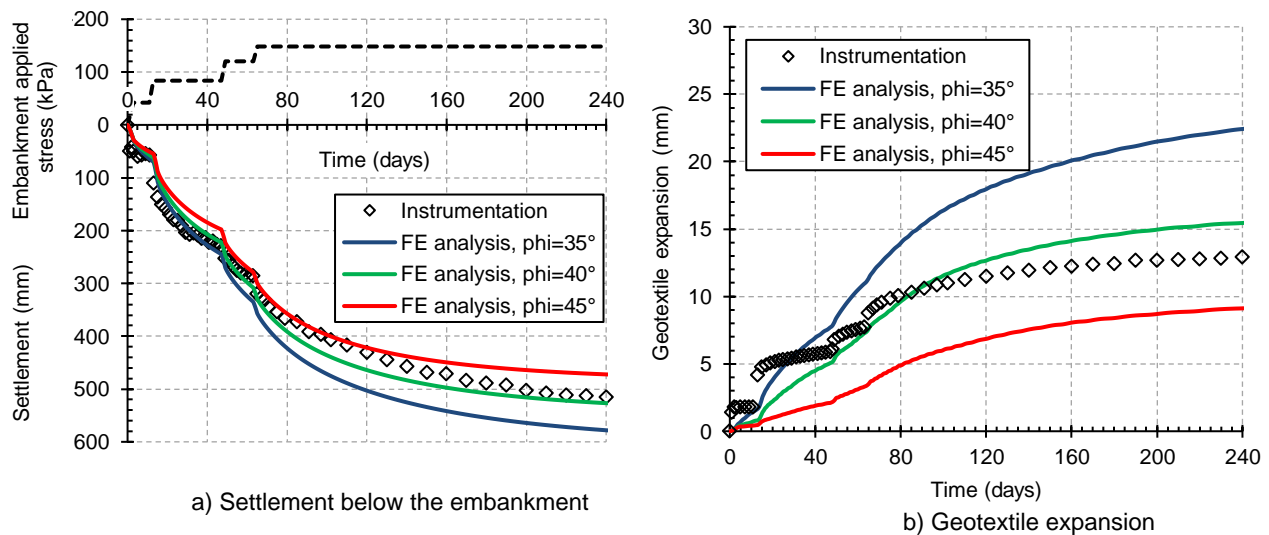


Figure 2. Influence of friction angle of the stone column material.

### 3.2 Influence of coefficient of earth pressure

In order to simulate the effect of the column installation, the parametric study was performed by varying the coefficient of at-rest earth pressure  $K_0$  using values equal to 0.8, 1.1 and 1.5. The coefficient of earth pressure in the natural repose for the soft clay I and soft clay II is 0.58 and 0.53, respectively. In Figure 3a, the increase in  $K_0$  leads to a significant reduction of embankment settlement, since the increase in the  $K_0$  coefficient generates a higher soil resistance against horizontal deformation. According to the results, increasing  $K_0$  coefficient from 0.8 to 1.5 causes the settlement at the end of the monitoring time (i.e. 240 days) to reduce from 500 mm to about 300 mm, an indirect evidence of the advantage of the displacement method on  $K_0$  improvement in the granular columns installation.

An increasing  $K_0$  coefficient increases the horizontal effective stress of the soft soil, which is practically the capacity of the soil to confine the column, resulting in a reduction of lateral expansion of the geotextile, as can be observed in Figure 3b. A remarkable reduction in column bulging (i.e. geotextile expansion) is seen when  $K_0$  coefficient is equal to 1.5 meaning the column is supported by a higher confining stress provided by the surrounding soft soil thus the column failure induced by the excessive bulging is less possible.

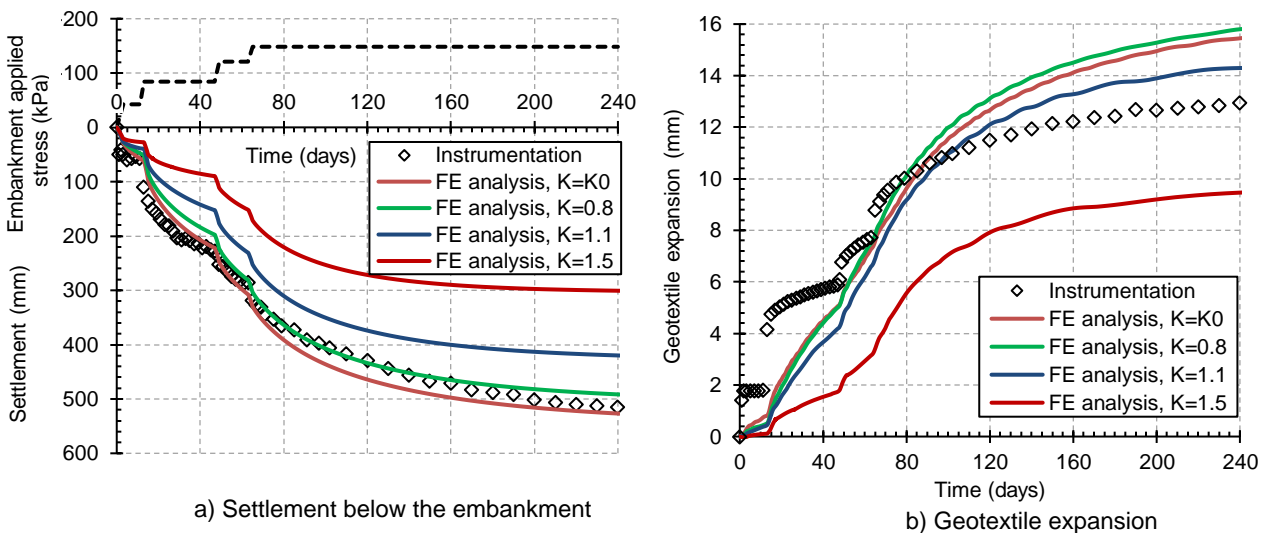


Figure 3. Influence of coefficient of lateral earth pressure.

### 3.3 Influence of column diameter (area replacement ratio)

The parametric study was done by varying the values of the diameter of the column  $d_c$  according to the commercial diameter of the geotextile encasement available in the market, so, the values chosen were 0.6, 0.8 and 1.0 m. The spacing between columns was maintained equal to 2 m, thus, these variations of the column diameter generate area replacement ratio values ( $a_c = d_c^2/d_e^2$ ) of 7%, 12.5% and 19.6%, respectively.

Figure 4a shows a clear reduction of the magnitude of the settlement as the diameter of the column  $d_c$  increases. A larger column diameter (i.e. higher  $a_c$  ratio) increases the percentage of the total load transferred directly on the top of the column thus the load transferred to the surrounding soil and the following settlement decrease. It is observed that increasing the column diameter from 0.6 to 1.0 m causes the magnitude of the final settlement to reduce about 34%. In addition, the time required for the settlement stabilization reduces with the increase of the column diameter. A 1.0 m-diameter column resulted in about 200 days of settlement stabilization, while the column with  $d_c = 0.8$  m took about 245 days and the column with  $d_c = 0.6$  m appears to have not reached stabilization at the end of the period analyzed. Castro and Sagaseta (2013) also reported that encased granular columns increase the consolidation coefficient of the soft clay hence reducing the time of settlement stabilization.

Figure 4b represents the geotextile expansion (i.e. column bulging) as a function of time for three different values of column diameter compared with measured data. It is clearly seen that the increased column diameter decreases the geotextile expansion. As the column bulging is associated with the settlement, the reduction of the settlement reduces the column

radial deformation. It may be observed that increasing the diameter of the column  $d_c$  from 0.6 m to 1.0 m causes nearly 60% reduction of the radial deformation.

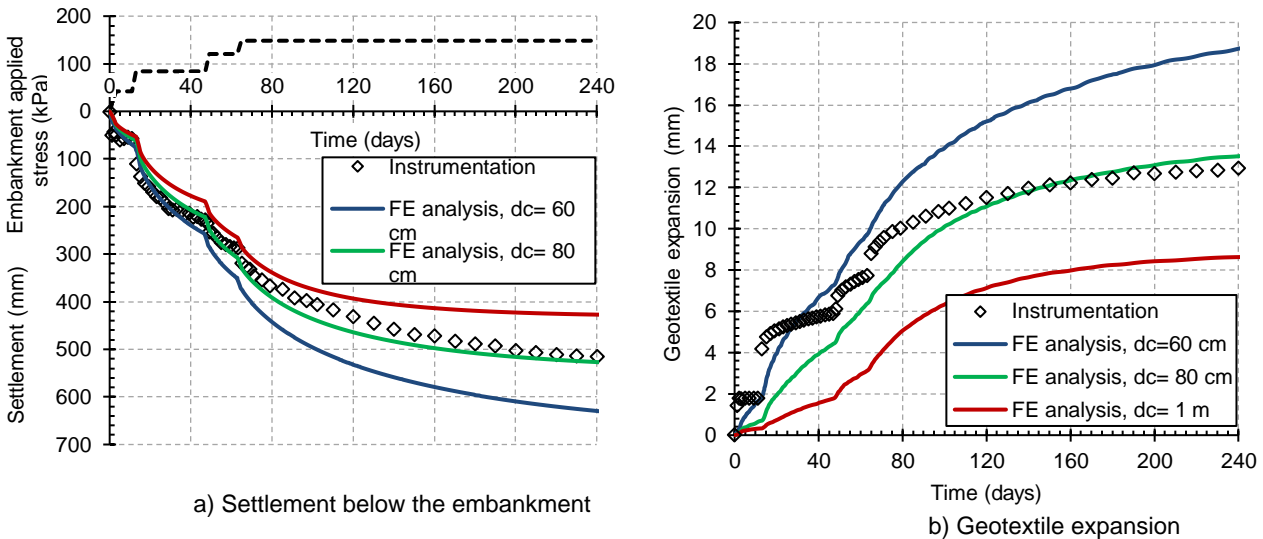


Figure 4. Influence of stone column diameter.

### 3.4 Influence of geotextile encasement stiffness

Values of the geotextile stiffness  $J$  used for the parametric analysis were close to the range available in the market equal to 875, 1750 and 3500 kN/m. Figure 5a shows the effect of increasing the modulus of stiffness of the geotextile on settlement development below the embankment centerline. It is clearly seen that an increase of the stiffness considerably reduces the magnitude of the settlement. For instance, increasing the geotextile stiffness from  $J = 875$  kN/m to  $J = 3500$  kN/m, decreases the final settlement (at 245 days) from 625 mm to about 410 mm. The higher confining support in the encased column provided by the stiffer geotextile is the reason of settlement reduction when the geotextile stiffness increases.

It is also observed that, for the larger geotextile stiffness ( $J = 3500$  kN/m), the settlement stabilizes at 160 days, while for the smaller geotextile stiffness ( $J = 875$  kN/m), the settlements have not yet stabilized at the end of analysis and yet tend to grow. According to numerical and analytical analyses (Castro and Sagasetta, 2013; Hosseinpour et al. 2014) the stiffer geotextile decreases the part of the load transferred to the soft soil, thus the excess pore pressure is smaller and the dissipation takes place faster.

As shown in Figure 5b, when a stiffer geotextile is used the column bulging reduces remarkably. Increasing the geotextile stiffness from  $J = 1750$  kN/m to  $J = 3500$  kN/m causes a 33% reduction of the column bulging at the end of monitoring time. It can also be noticed that the column horizontal displacement for the stiffer geotextile seems to stabilize at the end of the analyzed period (at 240 days), whereas for the other geotextile stiffness this yet tend to increase. This is due to the fact that the expansion is associated with the maximum settlement that occurs in the center of the embankment. As previously seen in Figure 5a the settlements for  $J = 3500$  kN/m have already stabilized, being in agreement with the results found for the expansion of the geotextile. It is observed, in general, that the geotextile stiffness has great an influence on the behavior of the encased column, presenting greater influence than the parameter of the column material.

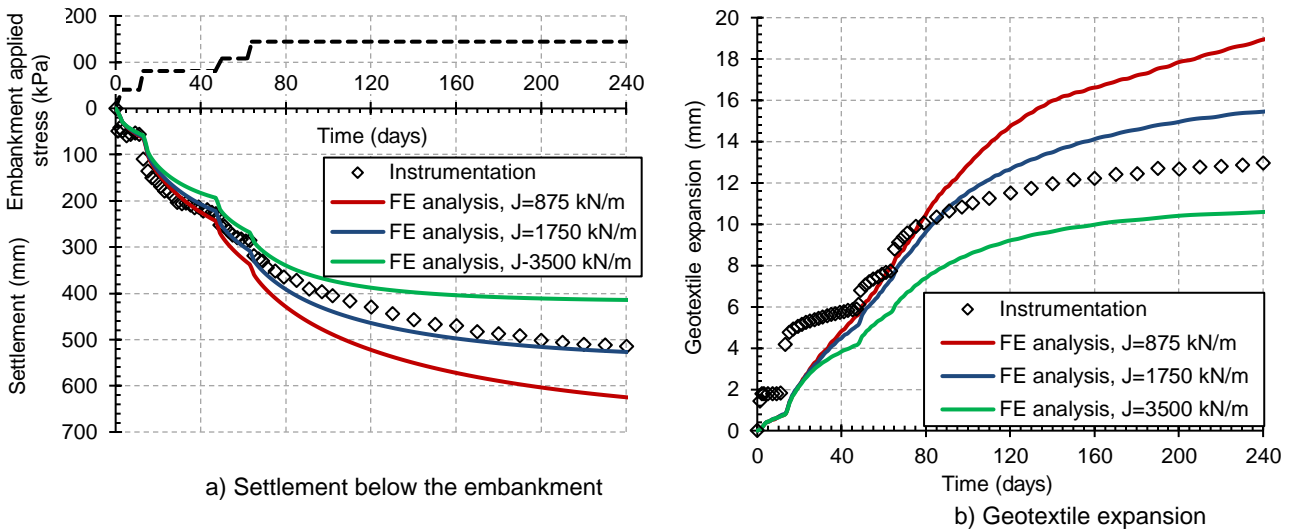


Figure 5. Influence of stiffness of geotextile encasement.

#### 4. DIFFERENTIAL SETTLEMENT

An important aspect for road or rail-road embankments over encased or un-encased granular columns is the differential settlement on the top of the embankment. McGuire et al. (2012) investigated differential settlements for the pile supported embankment and proposed a relationship to calculate the height required to avoid differential settlements (i.e. critical height) on the top of the embankments over rigid inclusions.

In this study, the numerical analyses are used to investigate the differential settlement for the test embankment over GEC. The geotechnical properties of the model are equal to those used in the parametric analyses. Four different values of area replacement ratio  $a_c$  are analyzed while the column spacing is kept constant equal to  $S= 1.76$  m resulting in different column diameters as presented in Table 2.

Table 2. Geometrical parameters used to study differential settlement.

Area replacement ratio, $a_c$ (%)	Columns' spacing, $S$ (m)	Column diameter, $d_c$ (m)
5	1.76	0.44
10	1.76	0.64
20	1.76	0.90
30	1.76	1.10

Figure 6 shows the variations of the differential settlements at the base and on the top of the embankment over GEC system for  $a_c$  values equal to 5, 10, 20 and 30% determined by numerical analysis. It is noticed that for any  $a_c$  values analyzed the differential settlement on the top of the embankment reduced as embankment height increased and the critical height was close to 1.5 m. The differential settlement at the base of the embankment; however showed a different variation and had a highest value for the lowest  $a_c$  ratio. Therefore, it can be stated that unlike the differential settlement on the top of the embankment, the differential settlement at the base is associated with the area replacement ratio as a lower  $a_c$  value produced a higher differential settlement at the base of the embankment.

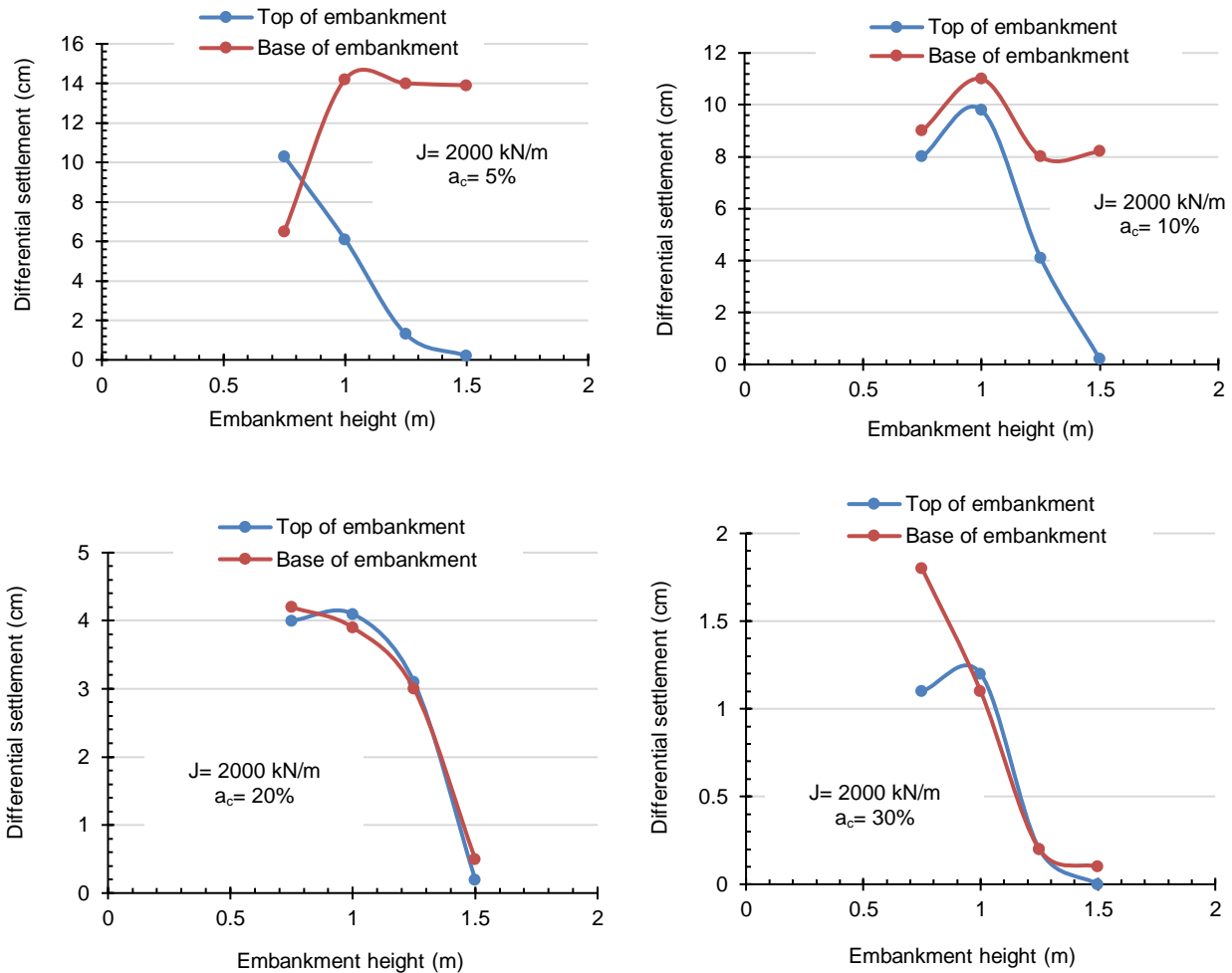


Figure 6. Differential settlements at the base and on the top of the embankment.

## 5. CONCLUSION

Finite element analysis was applied to study the settlement and column horizontal deformation for a test embankment over GEC system. Critical height of the test embankment was also analyzed and compared to the pile supported embankment. The main results are summarized as follow:

The higher column angle of friction  $\phi_c$  increases the shear strength of the encased granular column thus reduces both vertical and horizontal deformation. According to the results increasing  $\phi_c$  from  $35^\circ$  to  $45^\circ$  reduced column bulging to half, approximately.

An increase in  $K_0$  value results in a significant settlement reduction. The greater  $K_0$  value generates a higher soil resistance against horizontal deformation thus the capacity of the soil to confine the granular column improves and subsequently the column horizontal deformation reduces.

Increasing the granular column diameter (i.e. increasing  $a_c$  ratio) noticeably reduces either the settlement or the horizontal deformation. A larger column diameter enhances the percentage of the total load transferred on the top of the column thus the load on the surrounding soil and the following deformation decrease.

Stiffer geosynthetic encasement reduces the embankment settlement since it increases the granular column stiffness and thus its load bearing capacity. In addition, the column horizontal deformation reduces as it is encased with stiffer encasement due to higher confining stress provided by the geosynthetic encasement.

Unlike the top of the embankment, the differential settlement at base of the embankment was observed to be associated with the  $c_v$  values. The critical height for the present test embankment was also found to be equal to 1.5 m.

## REFERENCES

- Almeida, M.S.S., Riccio, M., Hosseinpour, I., and Alexiew, D. (2018). Geosynthetic encased columns for soft soil improvement, *CRC Press*, Taylor & Francis, London, UK.
- Almeida, M.S.S., Hosseinpour, I., Riccio, M. and Alexiew, D. (2015). Behaviour of geotextile-encased granular columns supporting test embankment on soft deposit, *Journal of Geotechnical and Geoenvironmental Engineering*, ASCE, 141(3): 04014116.
- Almeida, M.S.S., Hosseinpour, I. and Riccio, M. (2013). Performance of a geosynthetic-encased column (GEC) in soft ground: numerical and analytical studies, *Geosynthetics International*, 20(4): 252-262.
- Brinkgreve, R.B.J. and Vermeer, P.A. (2012). PLAXIS 2D: Finite element code for soil and rock analyses, Version 8.6, Balkema.
- Castro, J. and Sagaseta, C. (2013). Influence of elastic strains during plastic deformation of encased stone columns, *Geotextiles and Geomembranes*, 37: 45-53.
- Geng, L., Tang, L., Cong, S.Y., Ling, X.Z. and Lu, J. (2017). Three-dimensional analysis of geosynthetic-encased granular columns for liquefaction mitigation, *Geosynthetics International*, 24(1): 45-59.
- Hosseinpour, I., Almeida, M.S.S. and Riccio, M. (2017a). Verification of a plane strain model for the analysis of encased granular columns, *Journal of GeoEngineering*, 12(4): 97-105.
- Hosseinpour, I., Almeida, M.S.S., Riccio, M. and Baroni, M. (2017b). Strength and compressibility characteristics of a soft clay subjected to ground treatment, *Geotechnical and Geological Engineering*, 35(3): 1051-1066.
- Hosseinpour, I., Almeida, M.S.S. and Riccio, M. (2016). Ground improvement of soft soil by geotextile encased columns, *Proceedings of the Institution of Civil Engineers- Ground Improvement*, 169(4): 297-305.
- Hosseinpour, I., Riccio, M. and Almeida, M.S.S. (2014). Numerical evaluation of a granular column reinforced by geosynthetics using encasement and laminated disks, *Geotextiles and Geomembranes*, 42(4): 363-373.
- Khabbazian, M., Kaliakin, V.N., and Meehan, C.L. (2010). Numerical study of the effect of geosynthetic encasement on the behaviour of granular columns, *Geosynthetics International*, 17(3): 132-143.
- McGuire, M.P., Sloan, J., Collin, J. and Filz, G.M. (2012). Critical height of column-supported embankments from bench-scale and field-scale tests, *In: ISSMGE–TC 211, Intl. Symposium on Ground Improvement IS-GI*, Brussels, Belgium, CD-ROM.
- Murugesan, S. and Rajagopal, K. (2006). Geosynthetic-encased stone column: numerical evaluation, *Geotextiles and Geomembranes*, 24(6): 349-358.
- Raithel, M., Kempfert, H.G., and Kirchner, A. (2002). Geotextile encased columns (GEC) for foundation of a dike on very soft soils. *Proc. 7th Intl. Conference on Geosynthetics*, Nice, France, Balkema, 1025-1028.